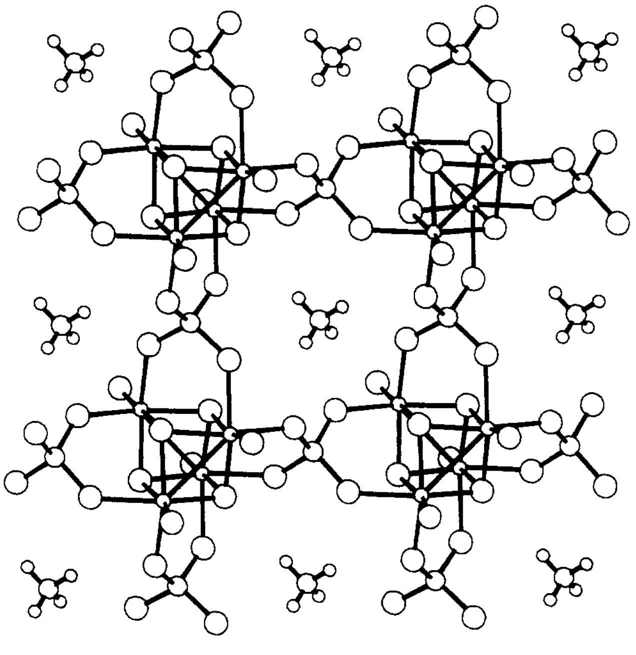

Figure 2. CHEMX (copyright, Molecular Design, Ltd.) generated view of $[N(C_3H_7)_4(NH_4)][(MoO)_4O_4(PO_4)_2]$ showing a layer of Mo_4O_8 groups joined through phosphate tetrahedra with ammonium groups centered in cavities within the layer (interlayer tetrapropylammonium groups omitted for clarity).

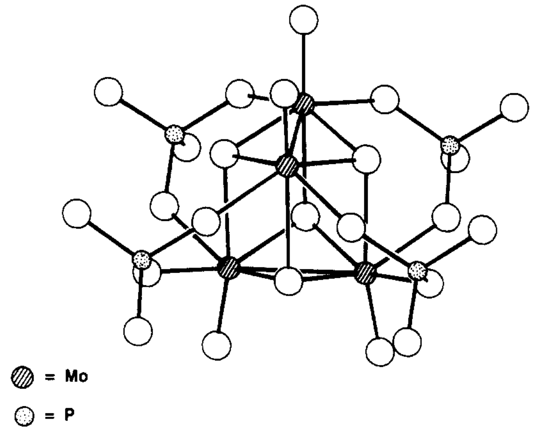

Figure 3. Illustration of the bonding in the Mo_4O_8 cube showing the four, triply edge-sharing Mo(V) octahedra. The octahedron is distorted because of a long Mo—O bond trans to a shorter Mo=O. There are two Mo–Mo single bonds per cube between edge-sharing Mo atoms; adjacent pairs of Mo atoms are connected to a common phosphate group through corner-shared oxygens. Overall, each Mo has two Mo–O–P linkages and a single Mo–Mo unit within its coordination sphere.

trans to a long (2.388 (6) Å) Mo—O bond; the four equatorial Mo—O bonds are similar in length (1.95–2.05 Å). This distortion of the octahedron is typical of other structurally characterized Mo(V) phosphates[6] and can be thought of in pronounced cases[6a] as a square-pyramidal arrangement of oxygen atoms around molybdenum. It is interesting to note that this bonding trend is also observed[7] for the cubane molybdenum(V) molecule $Mo_4O_8[(CH_3)_2POS]_4$. Pouchard[8] has proposed that the partial-double-bond character of the terminal oxo group is necessary for the stabilization of the d^1 state of Mo(V).

Estimation of the oxidation state of molybdenum in $[(MoO)_4O_4(PO_4)_2]^{2-}$ by summing the calculated[9] Mo–O bond strengths gives a value of +5.08, which is in good agreement with that based on stoichiometry. The four Mo(V) d^1 electrons in each cube pair to produce two metal-metal bonds (2.634 (2) Å) which form between edge-shared pairs of molybdenum atoms and are aligned parallel to the layers. This distance is similar to those reported for Mo–Mo bonds in $Cs_3Mo_4P_3O_{16}$,[5] $Cs_3Mo_5P_6O_{25}$,[10] and $Cs_3Mo_5P_7O_{24}$,[11] the only other examples of molybdenum phosphate structures containing metal-metal-bonded Mo_4O_4 cubes. It is also almost identical with that reported[7] for the molecular Mo(V)-oxygen cube $Mo_4O_8[(CH_3)_2POS]_4$, which has two Mo–Mo bonds of 2.635 Å and a geometry that is remarkably similar to that of the Mo_4O_8 subunit in $[(MoO)_4O_4(PO_4)_2]^{2-}$.

The reaction of molybdenum(VI) oxide with phosphoric acid normally leads to the formation of heteropoly anions, such as $[PMo_{12}O_{40}]^{3-}$, known as Keggin structures.[12] These molecules are avoided in the hydrothermal preparation of $[(MoO)_4O_4(PO_4)_2]^{2-}$ since the Mo(VI) common to these polyoxometalates is reduced (possibly by ammonium) to Mo(V) during the course of the reaction. Another, related molybdenum (V) phosphate has also been prepared in this manner by Haushalter et al.[13] Further synthetic investigations are in progress.

Acknowledgment. I thank A. J. Jacobson and J. W. Johnson for many helpful and informative discussions.

Supplementary Material Available: Tables of experimental details for the structure solution, atomic positional and isotropic equivalent thermal parameters, anisotropic thermal parameters, bond distances, and bond angles and an observed powder X-ray diffraction pattern (25 pages); a table of structure factors (3 pages). Ordering information is given on any current masthead page.

---

(6) (a) Kierkegaard, P.; Westerlund, M. *Acta Chem. Scand.* **1964**, *18*, 2217. (b) Minicheva, L. Kh.; Antsyshkina, A. S.; Lavrov, A. V.; Sakharova, V. G.; Nikolaev, V. P.; Porai-Koshits, M. A. *Zh. Neorg. Khim.* **1979**, *24*, 91. (c) Leclaire, A.; Monier, J.-C.; Raveau, B. *J. Solid State Chem.* **1983**, *48*, 147. (d) Lii, K.-H.; Haushalter, R. C. *J. Solid State Chem.* **1987**, *69*, 320. (e) Lii, K.-H.; Johnston, D. C.; Goshorn, D. P.; Haushalter, R. C. *J. Solid State Chem.* **1987**, *71*, 131. (f) Chen, J. J.; Lii, K.-H.; Wang, S. L. *J. Solid State Chem.* **1988**, *76*, 204. (g) Riou, D.; Goreaud, M. *J. Solid State Chem.* **1989**, *79*, 99.

(7) Mattes, R.; Mühlsiepen, K. *Z. Naturforsch.* **1980**, *35B*, 265.

(8) Pouchard, M.; Demazeau, G. Annual Meeting, Societe Chimique de France, 1982.

(9) Brown, I. D.; Wu, K. K. *Acta Crystallogr.* **1976**, *B32*, 1957.

(10) Lii, K.-H.; Haushalter, R. C.; O'Connor, C. J. *Angew. Chem., Int. Ed. Engl.* **1987**, *26*, 549.

(11) Wang, S.-L.; Lii, K.-H. *J. Solid State Chem.* **1988**, *73*, 274.

(12) Keggin, J. F. *Proc. R. Soc. London, A* **1934**, *144*, 75.

(13) Haushalter, R. C.; Lai, F. W.; Strohmaier, K. G. *Science*, in press.

Corporate Research Science Laboratories
Exxon Research & Engineering Company
Annandale, New Jersey 08801

Edward W. Corcoran, Jr.

Received September 6, 1989

Molecular Structure of $[nido\text{-}7,9\text{-}(CH_3)_2\text{-}7,9\text{-}C_2B_{10}H_{11}]^-$: The Kinetic Product Formed by Protonation of $[nido\text{-}(CH_3)_2C_2B_{10}H_{10}]^{2-}$

The $[nido\text{-}C_2B_{10}H_{12}]^{2-}$ anion, produced by the reduction of *closo*-$1,2\text{-}C_2B_{10}H_{12}$, provides a valuable synthon for many interesting and useful metallacarboranes.[1-5] The protonation of

---

(1) Dunks, G. B.; McKown, M. M.; Hawthorne, M. F. *J. Am. Chem. Soc.* **1971**, *93*, 2541.

(2) Dustin, D. F.; Dunks, G. B.; Hawthorne, M. F. *J. Am. Chem. Soc.* **1973**, *95*, 1109.

(3) Dustin, D. F.; Evans, W. J.; Jones, C. J.; Wiersema, R. J.; Gong, H.; Chan, S.; Hawthorne, M. F. *J. Am. Chem. Soc.* **1974**, *96*, 3085.

(4) (a) Salentine, C. G.; Hawthorne, M. F. *J. Am. Chem. Soc.* **1975**, *97*, 426. (b) Lo, F. Y.; Strouse, C. E.; Callahan, K. P.; Knobler, C. B.; Hawthorne, M. F. *J. Am. Chem. Soc.* **1975**, *97*, 428. (c) Salentine, C. G.; Hawthorne, M. F. *Inorg. Chem.* **1976**, *15*, 2872. (d) Salentine, C. G.; Hawthorne, M. F. *J. Chem. Soc., Chem. Commun.* **1975**, 848.

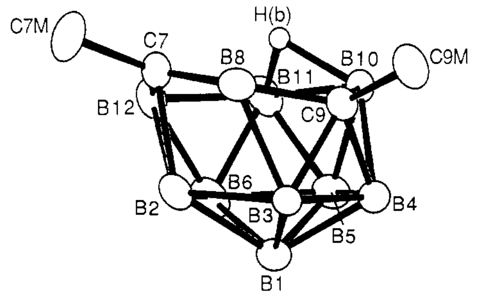

Figure 1. Molecular structure of the anion of **1**, [*nido*-7,9-$(CH_3)_2$-7,9-$C_2B_{10}H_{11}$]$^-$, with thermal ellipsoids drawn at 50% probability. All terminal hydrogen atoms have been omitted for clarity.

this anion results in the formation of two isomers:[6,7] an initially formed kinetic ("unstable") product and a thermodynamic ("stable") product. Two structural determinations of the thermodynamic product derived from the protonation of [*nido*-$R_2C_2B_{10}H_{10}$]$^{2-}$ anions (R = CH_3, C_6H_5) have been reported.[8,9] Both of these studies revealed the structure of the monoanions to be that of an icosahedron having one vertex removed and containing a methylene bridge: $CH(C_6H_5)$ or $CH(CH_3)$. While the "stable" isomer has little synthetic utility, since it is inert in the usual reactions leading to metallacarboranes,[5,10] the "unstable" isomer has been successfully employed in syntheses of metallacarboranes[5,10] and novel monocarbon carboranes.[11]

The structure of the "unstable" isomer has remained at the center of controversy. Several publications have predicted strictly deltahedral structures (the quadrilateral face, vide infra, was not considered to be a possibility), each based on then new information obtained via NMR techniques.[6,7,10] However, each of these predictions has now been proven to be incorrect. The correct structure of the kinetic product, as established by X-ray crystallographic techniques, is presented below.

The salt [$P(C_6H_5)_3CH_3$][*nido*-7,9-$(CH_3)_2$-7,9-$C_2B_{10}H_{11}$] (**1**) was prepared via the literature procedure.[6,7] Crystals of **1** were obtained by vapor diffusion of diethyl ether into a 1,2-dibromoethane solution of **1**. The solution was continuously refrigerated[12] (−10 °C) during the crystal growing process in order to prevent the rearrangement of **1** to the thermodynamic isomer.

The structure of **1** as determined by crystallographic means[13] is presented in Figure 1. It is derived from a (1,5,6,1) 13-vertex docosahedron with the vertex capping the hexagonal face removed. It very closely resembles the carboranyl fragment in the corresponding rhoda-,[10] cobalta-,[2,14] titana-,[4] pallada-,[5] and iridacarboranes.[5]

When the structure of **1** is compared with those of the carborane ligands of the metallacarboranes mentioned above, two features are apparent that make these compounds unique: the hexagonal face and the quadrilateral formed by B(2), C(7), B(8), and B(3). To facilitate comparisons, the carboranyl fragments in the five structurally characterized metallacarboranes have been renumbered to correspond directly with the numbering of **1**. In all of the carborane cages, the four boron atoms of the hexagonal face are coplanar and the carbon atoms are staggered, one above and one below this plane. This is most exaggerated in the case of **1**, where C(7) is 0.31 Å above the plane and C(9) is 0.32 Å below the plane. When the interatomic distances within the hexagonal face are compared, in the cobalta- and iridacarboranes the C(7)–B(8) distance is 1.429 (10) and 1.50 Å and the C(7)–B(12) distance is 1.527 (6) and 1.62 Å, respectively. This reveals asymmetry about C(7). However, in the case of **1**, these same distances are nearly symmetrical, with the C(7)–B(8) distance being 1.506 (7) Å and the C(7)–B(12) distance being 1.523 (7) Å. In the other metallacarboranes, these interactions are also short and nearly symmetrical about C(7) with an average difference of 0.020 Å. All of the remaining distances within the six-membered face of **1** are within the "normal" range for boron–boron distances or boron–carbon distances.[15]

The interatomic distances of the quadrilateral formed by B(2), C(7), B(8), and B(3) in **1** are as follows: B(2)–C(7), 1.796 (7) Å; C(7)–B(8), 1.506 (7) Å; B(8)–B(3), 1.858 (7) Å; B(3)–B(2), 1.892 (7) Å. The interatomic distances along the diagonals of this quadrilateral in **1** are as follows: B(2)–B(8), 2.093 (8) Å; B(3)–C(7), 2.816 (7) Å. It should be noted that the long diagonal, B(3)–C(7), of this quadrilateral is longest in **1**. The other diagonal, B(2)–B(8), is longest in the iridacarborane. The remaining distances about the quadrilateral of **1**, with the exception of C(7)–B(8) (see above), are not noteworthy. The remainder of the interatomic distances and angles within **1** are normal and are given in the supplemental materials.

The precise mechanism by which **1** isomerizes to the "stable" isomer is not known. However, the driving force for the rearrangement of **1** to the "stable" isomer is apparent and involves the conversion of an acidic weakly held bridge proton to a very

---

(5) Alcock, N. W.; Taylor, J. G.; Wallbridge, M. G. H. *J. Chem. Soc., Dalton Trans.* **1987**, 1805.

(6) Dunks, G. B.; Wiersema, R. J.; Hawthorne, M. F. *J. Chem. Soc., Chem. Commun.* **1972**, 899.

(7) Dunks, G. B.; Wiersema, R. J.; Hawthorne, M. F. *J. Am. Chem. Soc.* **1973**, *95*, 3174.

(8) (a) Tolpin, E. I.; Lipscomb, W. N. *J. Chem. Soc., Chem. Commun.* **1973**, 257. (b) Tolpin, E. I.; Lipscomb, W. N. *Inorg. Chem.* **1973**, *12*, 2257.

(9) Churchill, M. R.; DeBoer, B. G. *Inorg. Chem.* **1973**, *12*, 2674.

(10) (a) Hewes, J. D.; Knobler, C. B.; Hawthorne, M. F. *J. Chem. Soc., Chem. Commun.* **1981**, 206. (b) Hewes, J. D. Ph.D. Dissertation, University of California at Los Angeles, 1984.

(11) Plesek, J.; Jelinek, T.; Stibr, B.; Hermanek, S. *J. Chem. Soc., Chem. Commun.*, **1988**, 348.

(12) During the early stages of this process, before any crystals had appeared, the solution was periodically removed from the refrigerator and warmed slightly by hand in order to melt the 1,2-dibromoethane and allow it to be diluted by the ether. After this procedure had been performed twice, the freezing point of the solution had been sufficiently lowered that it no longer froze at −10 °C. The solution was allowed to stand undisturbed for a period of 1 week, after which crystals were visible on the sides of the vessel. Several of these crystals were quickly mounted on glass fibers at room temperature and stored in the refrigerator until the diffractometer was available for data collection.

(13) Crystallographic data for **1**: temp/K, 128; wavelength/Å, 0.7107; space group, $P2_1/n$; a/Å, 11.844 (1); b/Å, 15.813 (2); c/Å, 14.630 (2); β/deg, 104.753 (4); V/Å^3, 2650; Z, 4; ρ(calcd)/g cm^{-3}, 1.13; μ/cm^{-1}, 1.1; R, 0.056; R_w, 0.068; GOF, 2.02. Collection and reduction of X-ray data for **1**: A colorless crystal, obtained from a $C_2H_4Br_2$ solution, was mounted on a thin glass fiber on a modified Picker FACS-1 diffractometer. Unit cell parameters were determined from a least-squares fit of 31 accurately centered reflections ($9.8 < 2\theta < 20.1°$). These dimensions and other parameters, including conditions of data collection, are summarized in Table I of the supplemental material. Data were collected at 128 K in the θ–2θ scan mode. Three intense reflections ($02\bar{3}$, 221, 060) were monitored every 97 reflections to check stability. Intensities of these reflections fluctuated ca. ±2.2%, with no decay, during the course of the experiment (46.1 h of exposure). Of the 3463 unique reflections measured, 2357 were considered observed ($I > 3\sigma(I)$) and were used in the subsequent structure analysis. Data were corrected for Lorentz and polarization effects. Programs used in this work include locally modified versions of the following programs: CARESS (Broach, Coppens, Becker, and Blessing), peak profile analysis, Lorentz and polarization corrections; ORFLS (Busing, Martin, and Levy) and SHELX76 (Sheldrick), structure factor calculations and full-matrix least-squares refinement; MULTAN80 (Woolfson et al.), statistical methods; ORTEP (Johnson). Solution and refinement of the structure of **1**: Atoms were located by use of MULTAN80. All calculations were performed on the VAX 11/750 crystallographic computer. Anisotropic thermal parameters were refined for all nonhydrogen atoms. The phenyl rings were treated as rigid groups: C–C = 1.39 Å; C–H = 1.0 Å; angles = 120°. All hydrogen atoms on carbon were kept in calculated positions (methyl H, C–H = 1.0 Å, H–C–H = 109.5°). Positional parameters were refined for the hydrogen atom bridging the two boron atoms. All other hydrogen atoms bonded to boron were kept in located positions. Isotropic thermal parameters, u, for H were set at 0.035 for all non-methyl hydrogens. These parameters were set at 0.06, 0.05, and 0.04 for hydrogen on C(7M), C(9M) and C(41), respectively. Scattering factors for H were obtained from Stewart et al. (Stewart, R. F.; Davidson, E. R.; Simpson, W. T. *J. Chem. Phys.* **1965**, *42*, 3175) and for other atoms were taken from: *International Tables for X-ray Crystallography*; Kynoch Press: Birmingham, England, 1974; Vol. IV. Anomalous dispersion terms were applied to the scattering of P. The largest peaks on a final difference electron density map were ±0.3 e Å^{-3}. Final positional and thermal parameters for nonhydrogen atoms are given in Table II of the supplemental material.

Inorg. Chem. **1990**, *29*, 160-167

stable terminal C-H bond accompanied by the conversion of the cage geometry to one possessing only triangular faces.

The determination of the structure of **1** renews our interest in the structure of the dianion [*nido*-$C_2B_{10}H_{12}$]$^{2-}$. On the basis of the structure of **1** and those of the metallacarboranes containing the $[C_2B_{10}H_{12}]^{2-}$ ligand, it is anticipated that the structure of the dianion is similar to that of **1**, with the bridge proton removed. Due to the highly fluxional nature of [*nido*-$C_2B_{10}H_{12}$]$^{2-}$, its structure can only be determined with certainty via X-ray diffraction methods. Attempts to accomplish this are in progress.

Acknowledgment. The support of this work by the National Science Foundation (Grant CHE-88-06179) is gratefully acknowledged.

Supplementary Material Available: Listings of crystallographic data (Table I), positional and thermal parameters (Table II), interatomic distances and angles (Table III), distances within the hexagonal faces of the referenced metallacarboranes and **1** (Table A), and distances within the quadrilateral formed by C(7), B(2), B(3), and C(8) of the referenced metallacarboranes and **1** (Table B) (7 pages); a listing of calculated and observed structure factors (Table IV) (13 pages). Ordering information is given on any current masthead page.

---

(14) Churchill, M. R.; DeBoer, B. G. *Inorg. Chem.* **1974**, *13*, 1411.

(15) Mastryukov, V. S.; Dorofeeva, O. V.; Vilkov, L. V. *Russ. Chem. Rev. (Engl. Transl.)* **1980**, *49*, 1181.

Department of Chemistry and
Biochemistry
University of California
Los Angeles, California 90024-1569

Thomas D. Getman
Carolyn B. Knobler
M. Frederick Hawthorne*

Received October 5, 1989

Articles

Contribution from the Department of Chemical and Biological Sciences,
Oregon Graduate Center, Beaverton, Oregon 97006-1999

Structure and Water-Oxidizing Capabilities of Dimeric Ruthenium EDTA Complex Ions

Jinzhong Zhou, Wu Xi, and James K. Hurst*

Received April 18, 1989

Low-temperature resonance Raman (RR) spectra of the dimeric $Ru^{III}Ru^{IV}$ ion formed by oxidation of $Ru(edta)OH_2^-$ exhibited a prominent band at 433 cm^{-1}, which shifted to 431 cm^{-1} upon substitution of $[^{18}O]$-H_2O in the primary coordination sphere of the precursor ion. A second band, at 324 cm^{-1}, underwent a comparable isotope-dependent shift to lower energies. The RR spectra were insensitive to deuterium substitution. These features establish that the dimer is a μ-oxo ion, i.e., $[Ru(edta)]_2O^{3-}$; from the magnitude of the isotopic shifts, the Ru-O-Ru angle was estimated to be 165°. The reduction potential for the $Ru^{IV}{}_2/Ru^{III}Ru^{IV}$ couple was acid-insensitive over the range pH 2-11, suggesting that the dimer does not contain coordinated H_2O in either oxidation state. Cyclic voltammographic results in neutral solution suggested that $[Ru(edta)]_2O^{2-}$ was unstable with respect to decomposition. A reinvestigation of the water-oxidizing capabilities of this ion by polarographic, gas chromatographic, and mass spectrometric methods failed to reveal O_2 among the gaseous products. Instead, copious quantities of CO_2 were formed, the source of which was coordinated EDTA.

Binuclear ions form upon oxidation of $Ru(edta)(OH_2)^-$ in aqueous solution. Numerous structures have been proposed for the dimers including, in early studies, $L_2Ru^{IV}{}_2$ or mixed-valent $L_2Ru^{III}Ru^{IV}$ ions that are either doubly bridged by dihydroxo, peroxo and hydroxo, superoxo and hydroxo, or aqua and oxo ligands.[1,2] More recently, redox titrations with several oxidants have established that the stable dimeric product is a mixed-valent ion,[3,4] formally $L_2Ru^{III}Ru^{IV}$, although its optical and magnetic properties are indicative of an electronic ground state in which the unpaired spin density is strongly delocalized over both metal centers.[4] Furthermore, the stoichiometry of proton release accompanying oxidation in weakly acidic solutions is consistent only with μ-oxo or dihydroxy ligand bridging.[4] Baar and Anson also proposed conversion to a mixed hydroxo-oxo dibridging system in alkaline solution (pH >10), based upon the titrimetric behavior of the dimer and the pH dependence of the $L_2Ru^{III}Ru^{IV}/L_2Ru^{III}{}_2$ redox couple. They showed that the $L_2Ru^{III}Ru^{IV}$ ion could be further oxidized either chemically with Ce^{4+} or electrochemically to give a spectroscopically distinct species. From a Nernst plot of thin-layer spectroelectrochemical data, they ascertained that one-electron oxidation had occurred, yielding a $L_2Ru^{IV}{}_2$ ion. This latter species was unstable and spontaneously reverted to $L_2Ru^{III}Ru^{IV}$ or a spectroscopically indistinguishable ion. Reduction of the $L_2Ru^{IV}{}_2$ ion was thought to occur at the expense of solvent H_2O, on the basis of the observation of a positive response from a Clark polarographic electrode in the presence of excess Ce^{4+} ion or for solutions poised at a potential that allowed regeneration of the oxidized dimer.[4,5]

Our interest in this ion was prompted by the claim that it could act as a catalyst for water oxidation. Several μ-oxo ruthenium dimers of the type *cis,cis*-$[(bpy)_2Ru(OH_2)]_2O$ have been described that are capable of catalytically oxidizing water electrochemically or in the presence of strong oxidants.[6-9] Although the reaction mechanisms have not yet been identified, salient features are thought to include the presence of coordinated water, which provides access to higher oxidation states via deprotonation,[10] and the μ-oxo bridge, which, by forcing close juxtaposition of hydroxo or oxo ligands in the higher oxidation states, might facilitate reductive elimination of H_2O_2 or O_2.[6,7,9] Additionally, carboxyl

---

(1) Ezerskaya, N. A.; Solovykh, T. P. *Russ. J. Inorg. Chem. (Engl. Transl.)* **1968**, *13*, 96, and references therein.

(2) Taqui Khan, M. M.; Ramachandraiah, G. *Inorg. Chem.* **1982**, *21*, 2109.

(3) Ikeda, M.; Shimizu, K.; Sato, G. P. *Bull. Chem. Soc. Jpn.* **1982**, *55*, 797.

(4) Baar, R. B.; Anson, F. C. *J. Electroanal. Chem. Interfacial Electrochem.* **1985**, *187*, 265.

(5) Baar, R. B. Ph.D. Dissertation, California Institute of Technology, 1985.

(6) Gilbert, J. A.; Eggleston, D. S.; Murphy, W. A., Jr.; Geselowitz, D. A.; Gersten, S. W.; Hodgson, D. J.; Meyer, T. J. *J. Am. Chem. Soc.* **1985**, *107*, 3855.

(7) Raven, S. J.; Meyer, T. J. *Inorg. Chem.* **1988**, *27*, 4478.

(8) Rotzinger, F. P.; Munavalli, S.; Comte, P.; Hurst, J. K.; Grätzel, M.; Pern, F.-J.; Frank, A. J. *J. Am. Chem. Soc.* **1987**, *109*, 6619.

(9) Nazeeruddin, M. K.; Rotzinger, F. P.; Comte, P.; Grätzel, M. *J. Chem. Soc., Chem. Commun.* **1988**, 872.

(10) Meyer, T. J. *J. Electrochem. Soc.* **1984**, *131*, 221C.

0020-1669/90/1329-0160$02.50/0